Available online at www.sciencedirect.com

ScienceDirect

Procedia Structural Integrity 78 (2026) 2078–2085

Structural Integrity Procedia

www.elsevier.com/locate/procedia

XX ANIDIS Conference

Experimental investigation of tsunami waves-induced loads on a scaled building model

Maria Concetta Oddo[a,]*, Anthea Amato[a], Liborio Cavaleri[a]

[a]Universiy of Palermo, Viale delle Scienze, Edificio 8, Palermo, 90128, Italy

Abstract

In recent years, the scientific community has shown a growing interest in studying the effects that tsunami loads may involve on structures, as these powerful natural forces impact coastal regions with a certain recurrence. Especially after the Great Indian Ocean Tsunami event in 2004, researchers have shown an increasingly aware that tsunami risk is a real and significant threat that must be taken into consideration, given the immense destruction and loss of life that it can cause, as has already been demonstrated in past events. Against this background, numerous experimental, numerical, and analytical studies have been addressed to this topic, driven by the need to understand the full range of consequences that can result from hydraulic tsunami actions on structures. The results gained from these studies are intended to provide valuable insights to assist engineers in designing safer structure and infrastructure in areas prone to such extreme loading. Nevertheless, despite the recent efforts, the mechanisms through which tsunami forces interact with structures and infrastructures remain not fully understood. As well as, the available technical documents are still incomplete, and the methodologies proposed continue to be a subject of debate.
In the present study, some preliminary results of an experimental campaign conducted to investigate the response of a simplified two-storeys building model are presented and discussed. The experimental tests were carried out on a model, downscaled with a 1:25 ratio, subjected to tsunami wave action. These tsunami waves were generated in laboratory by a wavemaker inside a 2 × 2 × 40 m flow channel. In particular, these preliminary results refer to the high impact loading of focused waves on a scaled building model. The response of this building model was analyzed under varying inundation depths by measuring the time histories of forces. The results are discussed in detail and compared with the analytical formulations available in the literature.

Keywords: multi-hazard; tsunami vulnerability; bridges; Monte Carlo simulation; earthquake

* Corresponding author. Tel.: +39 3279156846.
E-mail address: mariaconcetta.oddo01@unipa.it

10.1016/j.prostr.2025.12.264

1. Introduction

Tsunamis are catastrophic natural events characterized by high-energy waves that can cause severe damage to buildings, infrastructure, populations, and economies. Global interest in tsunami research has increased significantly in recent years, driven in part by major events such as the 2004 Indian Ocean Tsunami (Ruangrassamee et al., 2006) and the 2011 Great East Japan Tsunami (Charvet et al., 2014). These disasters have highlighted the destructive potential of tsunami waves (data source: National Geophysical Data Center / World Data Service – NCEI/WDS Global Historical Tsunami Database).

Although recent tsunamis have occurred far from the Mediterranean region, the assumption that such events are unfamiliar to Italian coasts is misleading. Historical data confirm that tsunamis have impacted Italy in the past, as emphasized by Oddo et al. (2024), underscoring the need for increased regional awareness and preparedness.

A global review of tsunami occurrences by Reid and Mooney (2023) reports that approximately 67% of tsunamis in the Mediterranean region have been caused by earthquakes. More broadly, the review indicates that about 80% of tsunamis worldwide are triggered by seismic activity, although other natural phenomena, such as landslides and volcanic eruptions, can also contribute to their occurrence. On this background, numerous studies have focused on structural vulnerability assessment and tsunami risk mitigation (Foytong and Ruangrassamee, 2016). These efforts have integrated technical knowledge, guidelines, and protocols that are essential for understanding, preparing for, and responding to tsunami events. Notably, the FEMA P646 (2012) document offers detailed technical guidance for designing tsunami-resistant structures, including criteria for calculating tsunami loads and identifying structural systems suitable for vertical evacuation facilities. In addition to the FEMA guidelines, both analytical and experimental studies have been conducted in recent years to refine tsunami force estimation. Analytical models have increasingly been developed by incorporating findings from laboratory experiments to better quantify tsunami forces and their dependence on various parameters (Rossetto et al. 2011, Shafiei et al. 2016). For example, Qi et al. (2014) and Foster et al. (2017) examined the forces acting on rectangular structures in both steady and unsteady free-surface channel flows. Their studies aimed to empirically determine the drag coefficient (C_D) and the hydrostatic coefficient (C_H), which are included in the calculation of the hydrodynamic and hydrostatic forces as defined in FEMA P646 (2012) and ASCE 7 (2017). According to these studies, the drag coefficient is obtained to be approximately $C_D = 1.9$ for unbounded (turbulent) flow, and $C_D = 2.1$ for non-turbulent flow. While the hydrostatic coefficient was estimated at $C_H = 0.58$. Wüthrich et al. 2018, focused on the loading process for free-standing buildings, particularly the hydrodynamic behavior during wave impact. Their studies examined how openings in the structure and the presence of lateral or rear walls influence the resulting forces. They proposed analytical formulations calibrated to experimental results. For dry-bed surges, the horizontal force from the tsunami was expressed as proportional to the momentum flux per unit width (hu_m^2), where u_m is the depth-averaged flow velocity (used instead of peak velocity). Additionally, they replaced the drag coefficient C_D with a resistance coefficient C_R to better reflect the highly unsteady and rapidly changing nature of the wave impact. Unlike C_D, which is constant, C_R is time-dependent and more effective in capturing the dynamic characteristics of tsunami loading. An average value of $C_R = 2.0$ was found to be appropriate during the peak horizontal force, offering a more accurate representation of the dynamic impact. To simplify structural analysis, many studies focus primarily on hydrodynamic and hydrostatic forces. Fewer studies include impulsive forces in their analysis. According to Foster et al. (2017), impulsive forces may be neglected in some cases, and the theoretical framework proposed by Qi et al. (2014), originally developed for quasi-steady flow, can also be applied to certain unsteady inundation scenarios. The results of these studies show that in both steady and quasi-steady regimes, tsunami force estimation depends primarily on the Froude number and the building-to-flow width ratio. However, the rate of change in flow conditions has a limited effect on force parameterization.

In the present study, preliminary results from an experimental campaign are presented and discussed. Specifically, the response of a scaled model representing a two-storeys building subjected to tsunami loading is analyzed. Tsunami waves were simulated in a flow channel measuring 2×2×40 m, by generating focused waves characterized by three different significant inundation depths (0.10 m, 0.20 m, and 0.25 m). These focused waves were created by generating multiple wave components with varying frequencies and phases able to converge at a specific point in time and space. Focused waves were selected for this experimental campaign because they allow for the controlled reproduction of localized, high-energy wave events, representative of those occurring during real tsunami events. This configuration enables the accurate assessment of the peak loading conditions on structures under repeatable laboratory conditions. A data acquisition system was set to record the structural response and pressure distribution on the model, while external measurement systems (three probes) were used to monitor the wave heights. The results are presented as time histories of both the structural response and wave heights at the model location. Finally, the experimental data are compared with existing analytical formulations.

2. Experimental campaign

The experimental campaign was conducted in a wave channel for the reproduction of 2D wave phenomena, located at the Maritime Engineering Laboratory on the University of Palermo Campus. The experiments were carried out on a scaled model placed in the channel and subjected to different loading conditions, including solitary, focused, and irregular waves. However, the present study focuses solely on the effects of focused waves, characterized by three different significant wave heights: 0.10 m, 0.20 m, and 0.25 m. These focused waves are wave groups combined in such a way that they arrive in phase at a specific location, converging in a single, large wave crest that is significantly higher than the surrounding waves.

2.1. Laboratory set-up

The experimental set-up is illustrated in Fig. 1. The wave channel is 40 m long, 2 m wide, and 2 m deep. It is equipped on the right side with a modern wave maker capable of generating regular, irregular, and solitary waves. While, to reduce wave reflection, a passive absorption system is installed on the opposite (left) side.

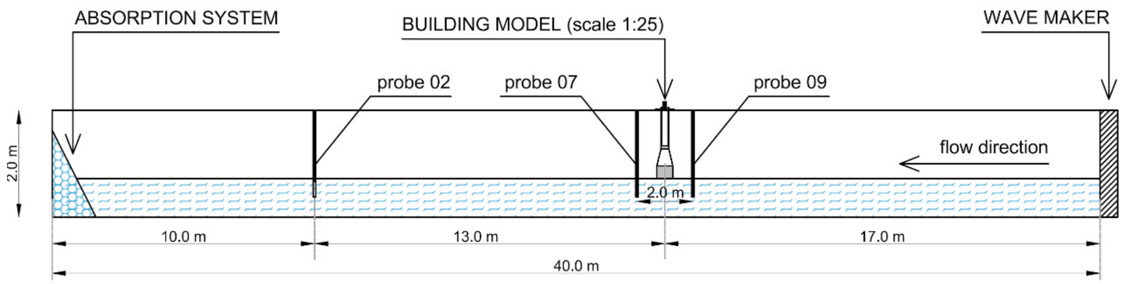

Fig. 1. Laboratory set-up: side view.

In this preliminary study, the channel platform representing the bathymetric profile was kept horizontal. The impact loading was investigated by analyzing the interaction between waves with varying inundation heights and a two-storeys building model, downscaled at a 1:25 ratio. The building model was placed 17 m from the wave maker, as shown in Fig. 1. To measure the water level before and after wave impact, three probes were installed along the channel. The first probe (Probe 09) was positioned 0.85 m in front of the model on the wave-facing side; the second (Probe 07) was placed 0.85 m behind the model. The third probe was installed 13 m further along the channel behind the model.

2.2. Model and data acquisition

The scaled building model has dimensions of 400 × 300 × 240 mm, see Fig. 2a. The longer side was positioned perpendicular to the flow direction to minimize additional force components and torsional effects that could arise from an oblique orientation surface of the model respect to the water flow. The building model was fixed to the side walls of the channel using a rigid steel frame, ensuring that its lower surface was aligned with the free water surface, set at a height of 72.5 cm, according to Fig. 2b. Forces and pressures were recorded during the experiment. Specifically, a tri-axial load cell with a capacity of 9000 N along the z-axis and 4500 N along the x- and y-axes was installed at the top of the model, as shown in Fig. 2a This set-up allowed for the measurement of the wave impact on the main surface, i.e. the shear resultant in the x-direction (Fx), the buoyant force (along the z-axis, Fz) as well as any unexpected effects, such as torsional moments (Mz), that may occur during test. Moreover, four pressure sensors were installed on the front face of the model, directly exposed to and impacted by the incoming wave, as shown in Fig. 2a.

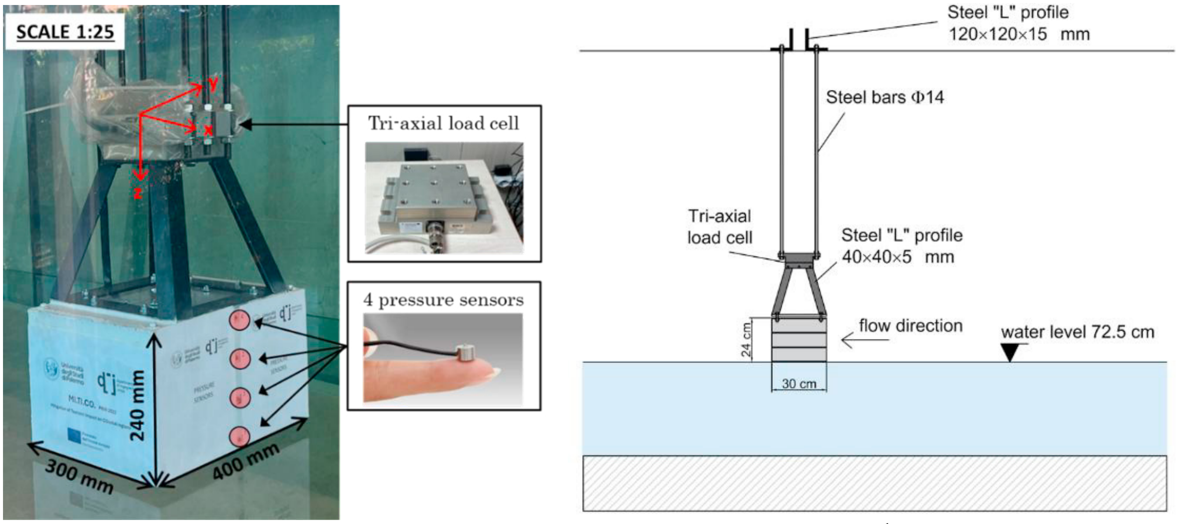

a b

Fig. 2. Building model (a) instrumentation with load cell and pressure sensors; (b) model configuration.

3. Available analytical formulations

The analytical formulations used in the structural design to estimate the hydrodynamic forces generated by tsunami action are often based on guidelines provided by the American Society of Civil Engineers (ASCE 7, 2017) and the Federal Emergency Management Agency (FEMA P646, 2012). According to these two documents, tsunami-induced loads consist of multiple, simultaneous or sequential force components. The first load acting on a structure is typically the impulsive force (F_i), which, as defined by both FEMA P646 (2012) and ASCE 7 (2017), is assumed to be 1.5 times the subsequent hydrodynamic force (F_d):

$$F_i = 1.5F_d \tag{1}$$

The hydrodynamic force (F_d) arises from moderate to high-velocity water flow impacting the structure and depends on fluid density, flow velocity, and the geometry of the structure. It is generally modeled as uniformly distributed pressure over the impacted surface.

$$F_d = \frac{1}{2}\rho \cdot B \cdot C_0 \cdot C_D \cdot \left(h \cdot u^2\right) \tag{2}$$

where ρ is the fluid density, C_D is the drag coefficient, measuring the resistance of an object in a fluid environment, C_0 is a coefficient accounting for the opening ratio of the impacted surface, B is the width of the impacted surfaces, h is the inundation depth, and u is the flow velocity. The hydrodynamic force (F_d) acts concurrently with the hydrostatic force (F_h), which contributes less to the overall loading after the wave impact. The hydrostatic force (F_h) acts perpendicular to the surface and is characterized by a pressure distribution that varies with the water depth relative to the structure or the surface of the structural element.

$$F_h = \frac{1}{2}\rho \cdot g \cdot B \cdot C_0 \cdot h^2 \tag{3}$$

begin g the gravitational acceleration.

Among the additional loads resulting from tsunami action are debris impact forces, debris damming effects, buoyant and uplift forces, and extra gravity loads from water retained on elevated floors. Although several experimental and analytical studies have been conducted in recent years to quantify the magnitude of these forces and evaluate how they interact with structures, determining an appropriate load pattern remains a significant challenge. For this reason, the present study considers only the formulations used to calculate impulsive, hydrostatic, and hydrodynamic forces.

4. Experimental results

Time histories of wave height and wave loads acting on the building model were recorded, setting an acquisition rate of 500 data/second for the tri-axial load cell and 100 data/second for the probes. A higher acquisition frequency was selected for the tri-axial load cell to accurately capture the impulsive actions. Fig. 3 presents the experimental results for the building model subjected to a focused wave with a significant wave height set at 0.25 m. Specifically, Fig. 3a shows the data in terms of shear load (T_x), buoyancy load (T_z), and torsional moment (M_z) recorded over a 150-second acquisition window, along with a zoomed-in view of the data from 24 to 60 seconds.

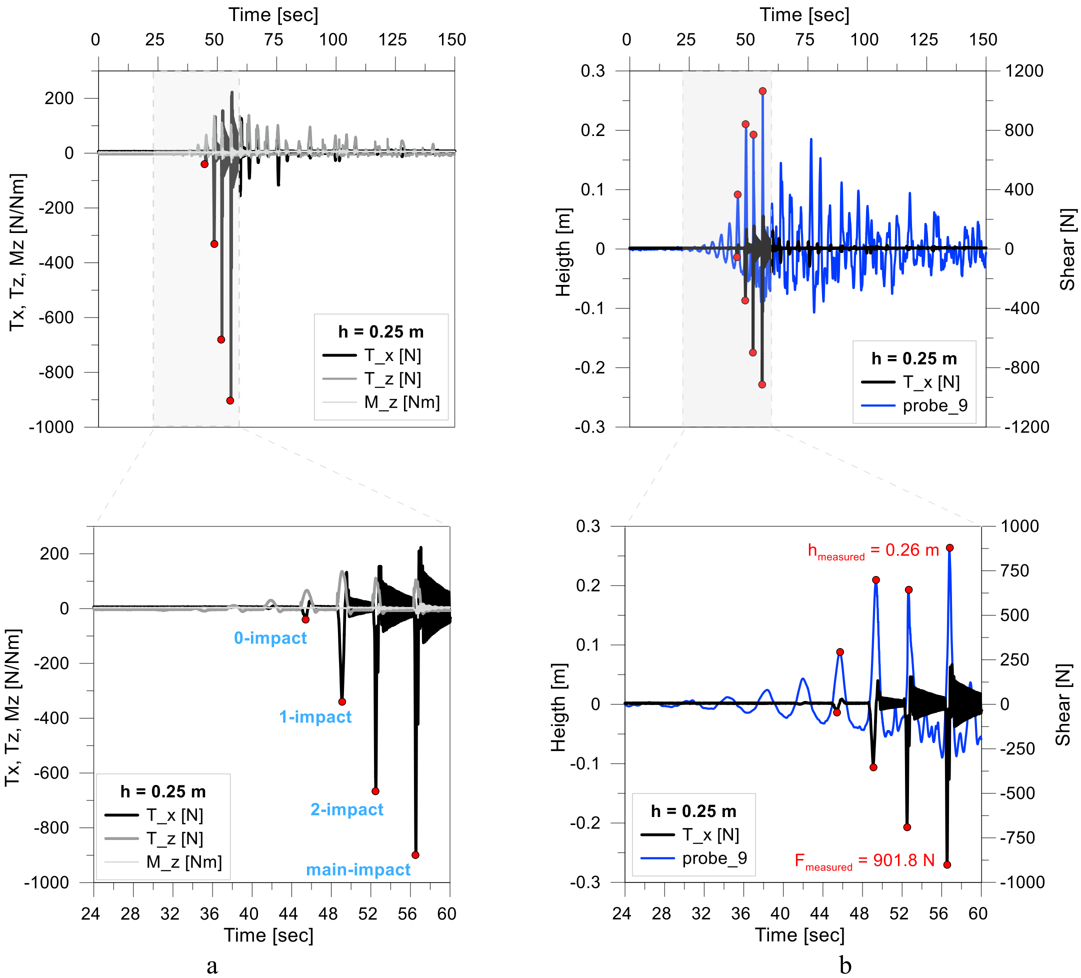

Fig. 3. Time history measurements at building model for wave height h = 0.25 m: (a) load cell data; (b) shear load vs wave height.

The results highlight that the dominant force component is the shear load (T_x). In addition, a vertical load (T_z) acting from the bottom to the top of the model is observed, representing a buoyancy effect caused by the local rise in water level when the wave impacts the structure. A small torsional moment (M_z) is also present, probably induced by asymmetric or non-uniform wave impact and localized turbulence around the structure. This unbalanced pressure distribution creates slight twisting forces around the vertical z-axis. However, this torsional component (M_z) is minor compared to the shear (T_x) and buoyancy forces (T_z), as shown in Fig. 3a, and can be reasonably considered negligible for the purpose of structural analysis. In Fig. 3b, the results in terms of shear load (T_x) are plotted alongside the wave height measurements obtained from Probe_9, which is positioned in front of the model, according to the scheme in Fig. 1. These results highlight that the focused wave, with a measured height of $h_{measured}$ = 0.26 m, is preceded by smaller "precursor" waves that strike the model before the main crest. These precursor waves generate shear load peaks when their heights approach h = 0.10 m (0-impact). Moreover, the magnitude of these shear load peaks increases progressively from the first precursor event (0-impact) to the third (2-impact), culminating in the largest peak at the main-impact.

The effects of the precursor waves preceding the main focused wave are less pronounced when the significant wave height is 0.10 m or 0.20 m. As shown in Fig. 4a and 4b, for the 0.10 m and 0.20 m cases, respectively, the precursor waves generate only minor shear loads on the model. These results suggest that the intensity of the wave-induced loads on the structure is probably influenced by the ratio between the wave height and the scale of the model. When this ratio is small, the impact of precursor waves becomes negligible, and the dominant response is primarily associated with the main focused wave.

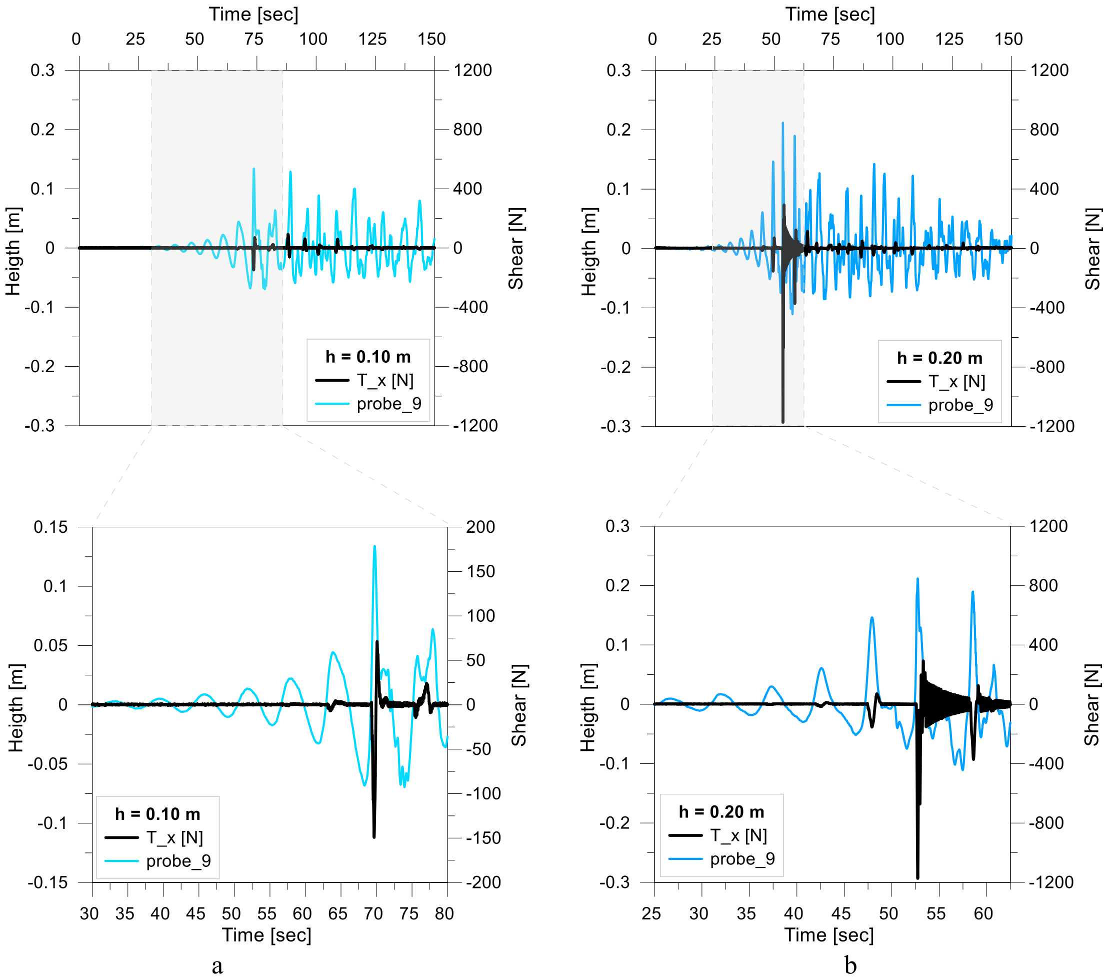

Fig. 4. Shear load vs wave height at building model: (a) for wave height h = 0.10 m; (b) for wave height h = 0.20 m.

4. Experimental vs analytical comparisons

Comparing the maximum measured shear loads (T_x) with the analytical values obtained using the formulations presented in the previous section, based on FEMA P646 (2012) and ASCE 7 (2017) guidelines, reveals some discrepancies. The experimental and analytical results are summarized in Table 1.

Table 1. Analytical and experimental results.

Significant focused wave height	Maximum measured wave height (probe_9)	Calculated flow velocity (u)	Calculated $F_h + F_d$	Calculated F_i	Measured peak load $F_{measured}$
0.10 m	0.13 m	2.29 m/s^2	176.2 N	211.5 N	149.5 N
0.20 m	0.21 m	2.88 m/s^2	441.0 N	529.2 N	1174.0 N
0.25 m	0.26 m	3.22 m/s^2	682.9 N	819.5 N	901.8 N

In particular, by examining the first two columns of Table 1, it can be observed that the settled significant focused heights generally do not correspond with the measurements obtained from probe 9, which is positioned in front of the model. The flow velocities used to calculate the hydrodynamic forces are determined according to the following equation (4), with the limitation that the Froude number is equal to 2. This assumption is justified by the fact that, in these experimental investigations where bathymetry effects are excluded, energy dissipation is ideally neglected. Consequently, the water flow propagates at the maximum velocity consistent with the Froude number assumption:

$$u = 2\sqrt{g \cdot h} \tag{4}$$

Analyzing the analytical results reveals that the sum of the hydrostatic and hydrodynamic forces (F_h + Fd) generally underestimates the measured peak loads, except in the case where h = 0.10 m. In this case, the ratio between the experimental and analytical forces ($F_{measured}$ / ($F_h + F_d$)) is approximately 0.9. However, when h = 0.25 m, this ratio increases to 1.3, and the ratio $F_{measured}$ / F_i reaches the value 1.1. These results suggest that, in general, when the flow velocity is lower, the impact load is comparable to the sum of hydrostatic and hydrodynamic forces ($F_h + F_d$), under the steady flow conditions. In contrast, as the velocity increases, the impact force becomes significantly more pronounced. It is worth noting that for h = 0.20 m, the measured peak load reached the value $F_{measured}$ = 1174.0 N, which exceeds both the analytically expected value ($F_h + F_d$) and the impulsive component F_i. This overestimation is probably due to an unexpected behavior observed after the wave impacts the model, specifically, the wave height increases (as shown in Fig. 5a) rather than decreases, as observed in the other test cases (Fig. 5b). This phenomenon was identified by comparing data from probe 9 (positioned in front of the model) and probe 7 (placed behind the model).

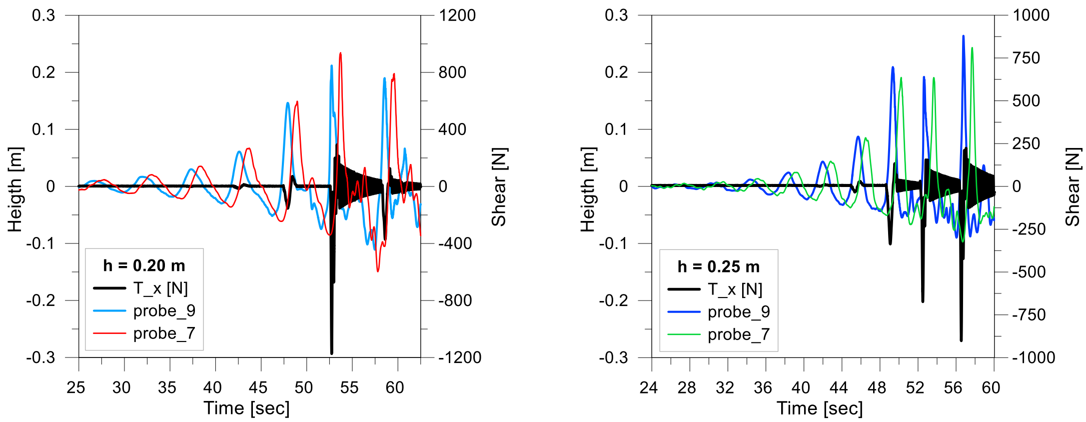

a b

Fig. 5. Comparison of shear load and wave height measurements from probes 9 (front of the model) and 7 (rear of the model): (a) for wave height h = 0.20 m; (b) for wave height h = 0.25 m.

The results suggest that the focused wave may have converged at a slightly different location and time than the ones initially planned. Such deviation could lead to a more concentrated energy transfer to the model, thereby amplifying the resulting load. These observations highlight the need for further investigation to better understand the operating conditions of the wave channel and to identify potential sources of disturbance that may affect the repeatability and accuracy of experimental tests.

5. Conclusions

This paper presents and discusses preliminary results from an experimental campaign conducted to investigate the effects of tsunami-induced loading on structures. Focused waves with heights of 0.10 m, 0.20 m, and 0.25 m were generated in a wave channel to simulate tsunami wave impacts.

The results indicate that the dominant load component acting on the structure is the shear force. A vertical load is also observed, representing the buoyancy effect as the wave interacts with the model. The experimental data, including maximum measured inundation depths and impact forces, are compared with the analytical predictions derived from the existing formulations. The comparisons reveal that, under conditions of high flow velocity, additional load components, potentially unaccounted for in the current analytical models, may significantly influence the structural response. Meanwhile, for low flow velocities, the measured response appears to align with the load combination expected under steady flow conditions.

These findings underscore the need for further investigation to validate or refine the preliminary results and to better understand the limitations of existing predictive models under extreme wave impact conditions.

Acknowledgements

This study was carried out within the PRIN 2022, cod. 2022YBAXTY_003, "MITICO - MIti-gation of Tsunami Impact on COstal regions", CUP B53D23006610006, and received funding from the European Union Next-Generation EU (National Recovery and Resilience Plan – NRRP, Mission 4, Component 2, Investment 1.1).

References

American Society of Civil Engineers (ASCE/SEI 7-16), 2017. Minimum Design Loads for Buildings and Other Structures, Reston, Virginia.

Charvet, I., Suppasri, A., & Imamura, F., 2014. Empirical fragility analysis of building damage caused by the 2011 Great East Japan tsunami in Ishinomaki city using ordinal regression, and influence of key geographical features. Stochastic Environmental Research and Risk Assessment, 28, 1853-1867.

Federal Emergency Management Agency (FEMA), 2012. Guidelines for Design of Structures for Vertical Evacuation from Tsunamis. (FEMA P-646). FEMA P-646 Publ.

Foytong, P., & Ruangrassamee, A., 2016. Fragility curves of reinforced-concrete buildings damaged by the 2004 tsunami. Engineering and Applied Science Research, 43, 419-423.

Foster, A. S. J., Rossetto, T., & Allsop, W., 2017. An experimentally validated approach for evaluating tsunami inundation forces on rectangular buildings. Coastal Engineering, 128, 44-57.

National Geophysical Data Center / World Data Service: NCEI/WDS Global Historical Tsunami Database. NOAA National Centers for Environmental Information. doi:10.7289/V5PN93H7.

Oddo, M. C., Asteris, P. G., & Cavaleri, L., 2024. Monte Carlo analysis of masonry structures under tsunami action: reliability of lognormal fragility curves and overall uncertainty prediction. In Structures (Vol. 63, p. 106421). Elsevier.

Qi, Z. X., Eames, I., & Johnson, E. R., 2014. Force acting on a square cylinder fixed in a free-surface channel flow. Journal of Fluid Mechanics, 756, 716-727.

Reid, J. A., & Mooney, W. D., 2023. Tsunami occurrence 1900–2020: A global review, with examples from Indonesia. Pure and Applied Geophysics, 180(5), 1549-1571.

Rossetto, T., Allsop, W., Charvet, I., & Robinson, D. I., 2011. Physical modelling of tsunami using a new pneumatic wave generator. Coastal Engineering, 58(6), 517-527.

Ruangrassamee, A., Yanagisawa, H., Foytong, P., Lukkunaprasit, P., Koshimura, S., & Imamura, F., 2006. Investigation of tsunami-induced damage and fragility of buildings in Thailand after the December 2004 Indian Ocean tsunami. Earthquake Spectra, 22(3_suppl), 377-401.

Shafiei, S., Melville, B. W., Shamseldin, A. Y., Adams, K. N., & Beskhyroun, S., 2016. Experimental investigation of tsunami-borne debris impact force on structures: Factors affecting impulse-momentum formula. Ocean Engineering, 127, 158-169.

Wüthrich, D., Pfister, M., Nistor, I., & Schleiss, A. J., 2018. Experimental study on the hydrodynamic impact of tsunami-like waves against impervious free-standing buildings. Coastal Engineering Journal, 60(2), 180-199.